Electrochemical and Solid-State Letters, **9** (1) A34-A38 (2006)
1099-0062/2005/9(1)/A34/5/$15.00 © The Electrochemical Society, Inc.

Effect of Capping Agents in Tin Nanoparticles on Electrochemical Cycling

Yoojung Kwon,[a] Min Gyu Kim,[b] Yoojin Kim,[a,b] Youngil Lee,[c] and Jaephil Cho[a,*,z]

[a]*Department of Applied Chemistry, Kumoh National Institute of Technology, Gumi, Korea*
[b]*Beamline Research Division, Pohang University of Science and Technology, Pohang, Korea*
[c]*Departmant of Chemistry, University of Ulsan, Ulsan, Korea*

Tin particles that were prepared using three different capping agents, hydrobenzamide, citrate, and polyvinyl pyrrolidone (PVP) exhibited different particle sizes. The hydrobenzamide-capped Sn had the smallest particle size (~50 nm) and uniform distribution while the citrate and PVP-capped Sn had particle sizes of ~100 and ~300 nm, respectively, with severe particle aggregation. However, there was no SnO_2 or SnO detected on the particle surfaces. The cycling results using coin-type half cells confirmed that the hydrobenzamide-capped Sn had the highest charge capacity of 994 mAh/g between 1.5 and 0 V and the best capacity retention. In contrast, the citrate and PVP-capped Sn showed severe capacity decay. Further analysis using cycled electrodes showed that the hydrobenzamide-capped Sn showed the least particle agglomeration and growth, compared with the others. From Fourier transform magnitude (FT) of Sn L_{III}-edge energy dispersive X-ray analysis spectra, these facts could be supported by the strong coordination formed as a result of chemical bonding between the nitrogen of the hydrobenzamide capping agent effectively inhibiting the particle growth during cycling.
 [DOI: 10.1149/1.2138447]

Manuscript submitted August 30, 2005; revised manuscript received October 4, 2005.
Available electronically November 21, 2005.

Nanoscale materials exhibit large surface areas and size-dependent distinct electronic, optical, magnetic, chemical thermal properties compared with their bulk counterparts.[1,2] For instance, nanomaterials, such as, CdSe, CdTe, Cu_2S, and Ag, Au, Co, Pd, Pt used capping agents to control the particle size and morphology. The properties of the protective ligands strongly influence the particle size and the dispersity of metal nanoparticles.[3] Nayral et al. reported that the synthesis of Sn/SnO_2 nanoparticles prepared by the decomposition of tin(II) amides, $Sn[(NMe_2)_2]_2$, at 135°C in dry-anisole-produced particles with a size <100 nm.[4] However, there was no evidence for Sn metal-phase formation provided, and the oxygen content was estimated from energy dispersive X-ray analysis (EDXA) to be 8 wt %. Yang et al. prepared C_4H_9-capped Sn nanoparticles by reacting $SnCl_4$ with Mg_2Sn in ethylene glycol dimethyl ether and followed by a reaction with n-C_4H_9Li. However, its X-ray diffraction (XRD) pattern clearly showed the large amount of SnO_2 contamination.[5] Still, these studies were aimed at sensors. Wang et al. reported that amorphous Sn and an Sn/SnO_2 core shell with particle sizes ranging from 3 to 7 nm could be prepared from a phenanthroline and a tin chloride complex. The oxygen content was estimated by X-ray photoelectron spectroscopy (XPS) analysis to be ~10 wt %.[6,7] However, no specific capacity data on Sn nanoparticles was provided. Recently, polyvinyl pyrrolidone (PVP) and citrate as capping agents were reported to play a key role in producing silver nanostructures with good stability and size/shape uniformity.[8-10] On the other hand, many other polymers such as poly(ethylene oxide) and poly(vinyl alcohol) failed.[10]

Many materials such as Si, Al, Sn, Sb, and Bi are capable of accommodating Li and show much higher Li storage capacities than those of carbonaceous materials.[11,12] Graphite can store 372 mAh/g corresponding to LiC_6, and tin can store 990 mAh/g corresponding to $Li_{4.4}Sn$. However, those metals show significant volume changes (>290%) that occur during Li alloying and dealloying, which causes cracking and crumbling of the electrode material and the consequent loss of electrical contact between the single particles, resulting in severe capacity loss.[13,14] Obtaining good capacity retention with alloy-negative electrodes is difficult, except when the capacity is constrained to values close to graphite. The reason for the failure is believed to be the inhomogeneous volume expansion in the coexistent regions of phases within the different lithium concentrations with the same particles, resulting in particle pulverization.[15-20] This is particularly true for coarse-grained, macrostructured metals. However, the level of mechanical strain can be reduced by tailoring the particle morphology of the Sn_xM_y (M = metals), particularly by employing smaller particle sizes.[21,22] Despite these efforts, Sn and tin alloys have not yet reached the reversible capacity

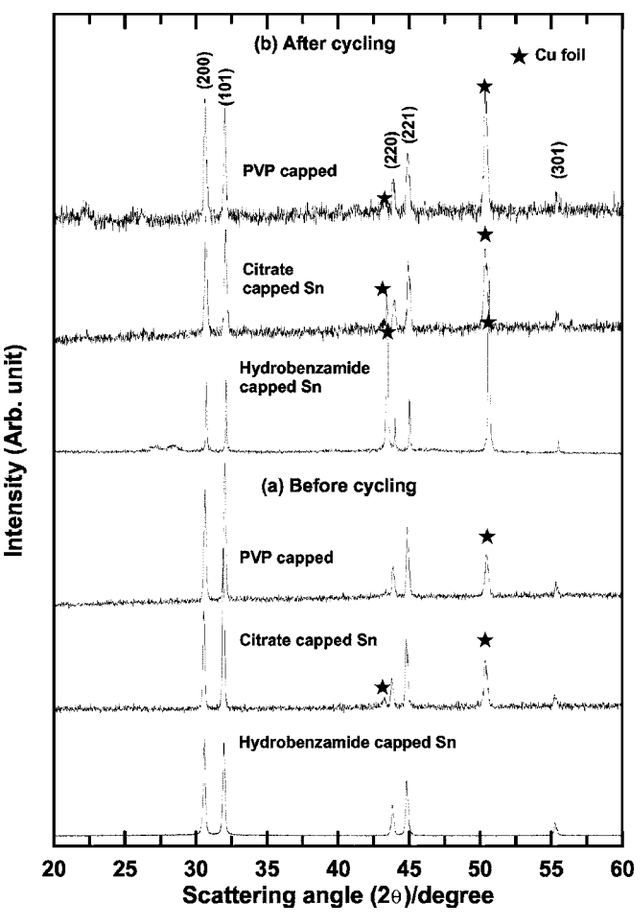

Figure 1. XRD patterns of the hydrobenzamide-, citrate-, and PVP-capped Sn anodes (a) before cycling and (b) after cycling.

* Electrochemical Society Active Member.
z E-mail: jpcho@kumoh.ac.kr

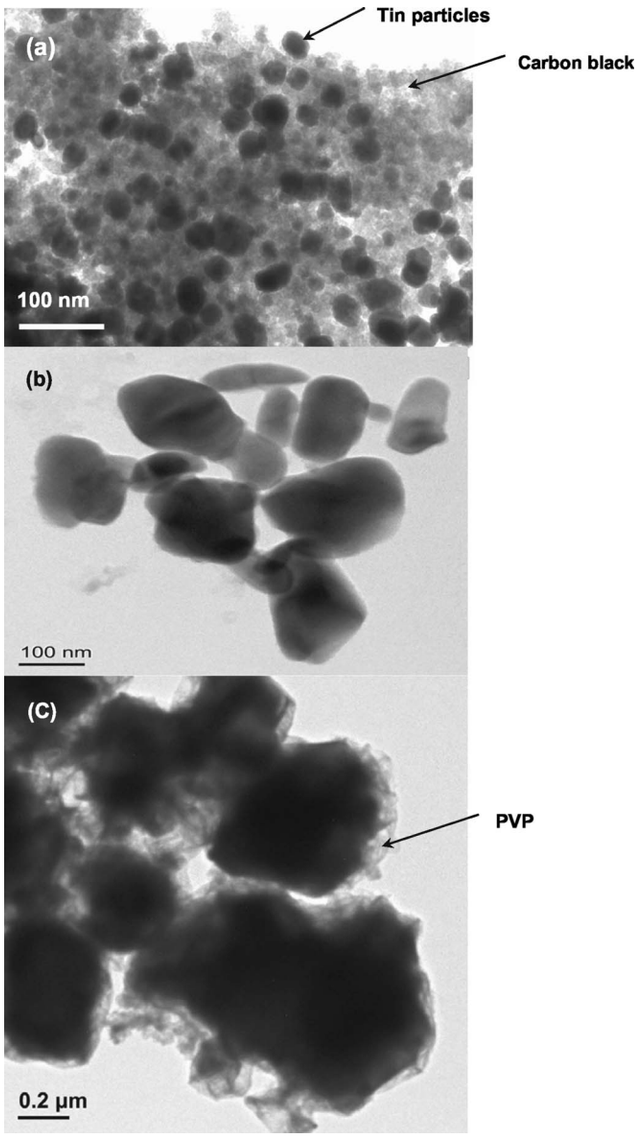

Figure 2. TEM images of the (a) hydrobenzamide-capped Sn nanoparticles (the powder was mixed with carbon black in NMP) (b) citrate capped-tin particles, and (c) PVP-capped tin particles.

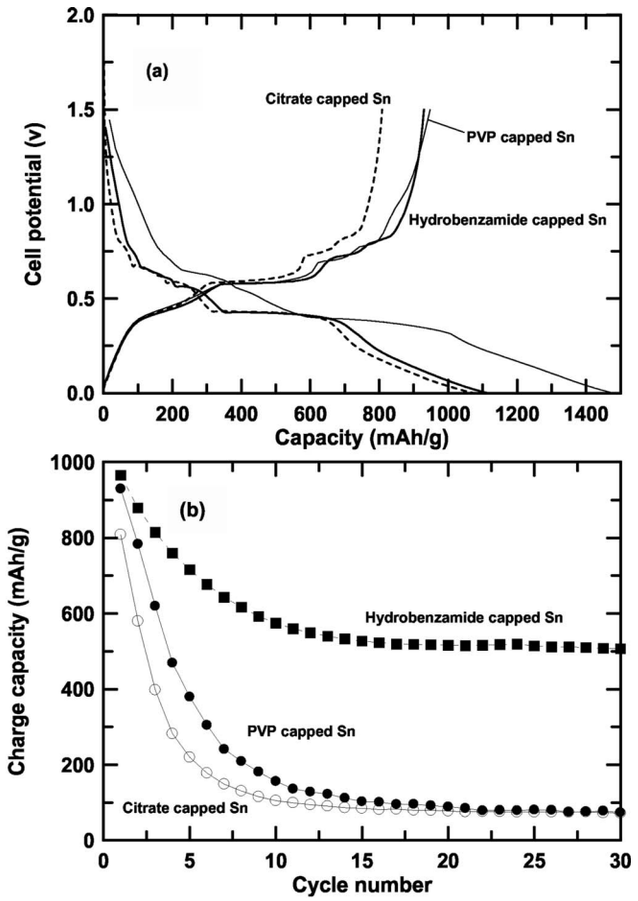

Figure 3. Plots of (a) first discharge and charge curves of the coin-type half cell containing hydrobenzamide-, citrate-, and PVP-capped Sn anodes between 1.5 and 0 V and (b) charge capacity vs cycle number in the coin-type half cell containing hydrobenzamide-, citrate-, and PVP-capped Sn anodes. C-rate used for the cycle test was 0.2 C (1 C = 900 mA/g).

of 900 mAh/g nor have they shown good capacity retention. Yang et al. reported that $Sn_{0.88}Sb_{0.12}$ particles <300 nm showed reversible capacity of 360 mAh/g even after 50 cycles, but they did not provide any evidence for particle-size distribution and Sn-phase formation.[23] $Sn_{0.88}Sb_{0.12}$ with a similar particle size to that reported above showed an initial capacity of 670 mAh/g. However, the capacity drastically decreased to 20 mAh/g after $\sim$30 cycles. Recently, Noh et al. reported that particles with $\sim$10 and 20 nm was controlled using new types of the capping agents, 2,4,6-tri(2-pyridyl)-1,3,5-triazine,3-(2-pyridyl)-5,6-diphenyl-1,2,4-triazine, respectively.[24] The results showed a retained reversible capacity of $>$900 mAh/g and 90% capacity retention after 30 cycles between 1.2 and 0 V. However, the drawback of these anodes is that the capping agents used are expensive and difficult to scale up.

This paper reports the synthesis and electrochemical properties of tin nanoparticles prepared using three different, cheap capping agents, PVP, citrate, and hydrobenzamide. In particular, hydrobenzamide is a much cheaper capping agent and shows better dispersion than 2,4,6-tri(2-pyridyl)-1,3,5-triazine, 3-(2-pyridyl)-5,6-diphenyl-1,2,4-triazine, which shows severe agglomeration of Sn colloidal particles.

Experimental

For preparing hydrobenzamide capped-tin metal particles, 1.17 mL of anhydrous $SnCl_4$ dissolved in 40 mL of 1.2-dimethoxyethane was mixed thoroughly with 3.0 g of hydrobenzamide dissolved in 30 mL of 1.2-dimethoxyethane. 0.75 g of $NaBH_4$, as a reducing agent, was also dissolved in 50 mL of 1.2-dimethoxyethane and poured into the mixed $SnCl_4$ solution. The mixture was stirred for 30 min at room temperature under an argon atmosphere. After the reaction, the mixture was washed four times with water and acetone and evaporated under vacuum to yield the tin particles. For preparing the citrate capped-tin particles, a 100 mL solution containing 27 g $SnCl_4{\cdot}5H_2O$ and 40.04 g of trisodium citrate was prepared in a conical flask (deoxygenized water was used as a solvent). $NaBH_4$, 6.97 g, was then added to the solution with vigorous stirring. The washing procedure was identical to that described above. The PVP-capped tin metal particles were prepared by adding 27.06 g of $SnCl_4{\cdot}5H_2O$ to deoxygenized water with vigorously stirring. PVP, 1.26 g, was dissolved in 40 mL of deoxygenized water, and poured into a mixed $SnCl_4{\cdot}5H_2O$ solution. Dissolved 4.5 g of $NaBH_4$, as a reducing agent in 50 mL deoxygenized water, was then added to the mixed solution. The mixture was stirred for

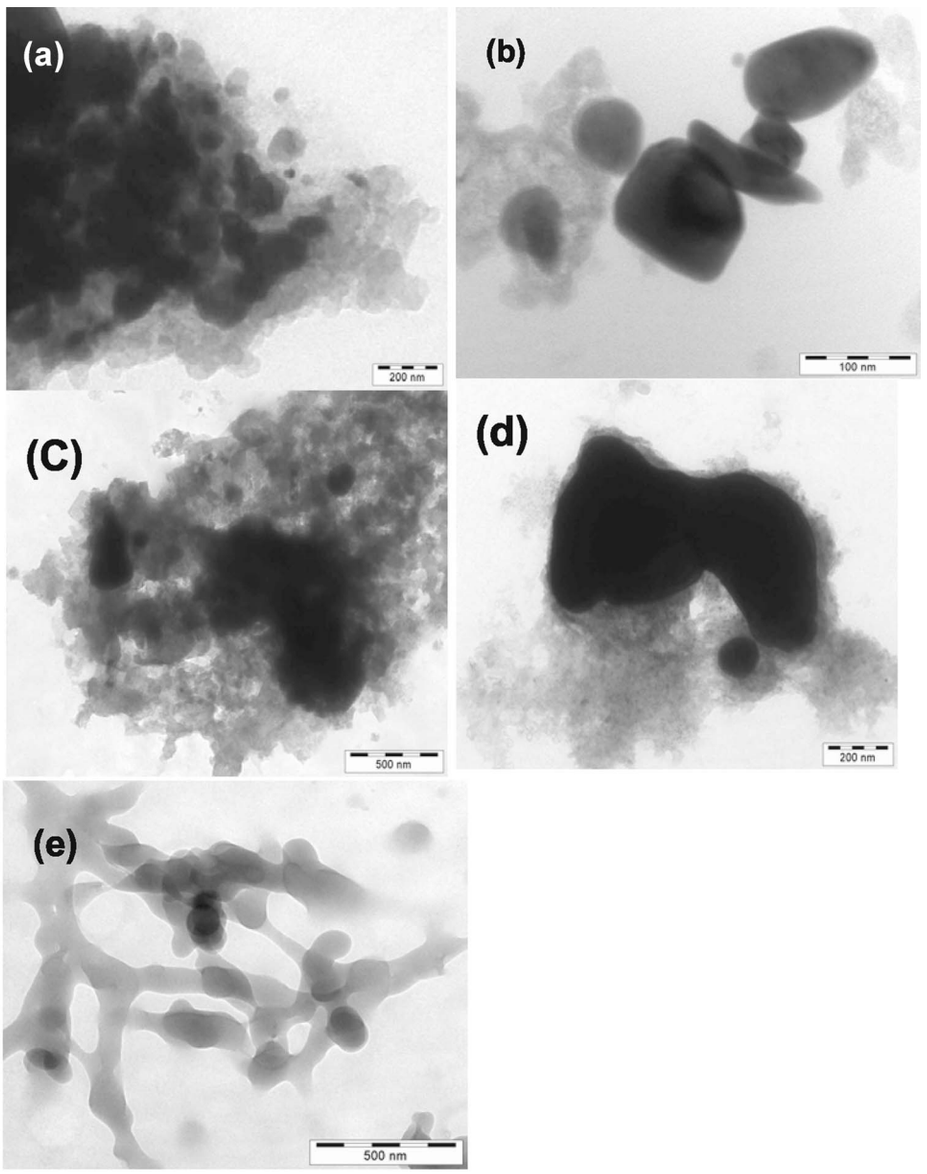

Figure 4. TEM images of the (a and b) hydrobenzamide-capped, (c) citrate-capped, and (d and e) PVP-capped tin electrodes after 30 cycles.

30 min at room temperature under an argon atmosphere. The resulting solution was stirred at 100°C for 30 min, and rinsed with deoxygenized water and acetone.

The electrochemical studies were carried out using coin-type half-cells (2016 type) with a Li counter electrode. A Sn nanoparticle:binder of carbon black in a weight ratio of 8:1:1 was used as the working electrode. The working electrode was made from the active material, Super P carbon black (MMM, Belgium), and polyvinylidene fluoride (PVDF) binder (Kureha, Japan). The electrodes were prepared by coating a slurry onto a Cu foil followed by drying it at 110°C for 20 min. The slurry was prepared by thoroughly mixing a *N*-methyl-2-pyrrolidone (NMP) solution of PVDF, carbon black, and the powdery active material. The coin-type battery test cells (size 2016R) that were prepared in helium-filled glove box contained a cathode, a Li metal anode, and a microporous polyethylene separator. The electrolyte was 1 M $LiPF_6$ with ethylenecarbonate/diethylenecarbonate/ethyl-methylcarbonate (EC/DEC/EMC) (30:30:40 vol %) (Cheil Industry, Korea). We used standardized coin-cell parts (2016R-type), and the amount of the electrolyte was normally ~0.1 g in each cell. After cycling, the tin particles were separated from the composite electrode using ultrasonic rinsing in acetone and centrifugation.

Results and Discussion

Figure 1 shows the XRD patterns of the hydrobenzamide, citrate, PVP-capped Sn particles, showing the formation of an orthorhombic β-Sn phase. The calculated particle sizes using Scherrer's formula were 160, 90, and 50 nm for the PVP, citrate, and hydrobenzamide-capped tin nanoparticles, respectively. Figure 2 shows transmission electron microscopy (TEM) images of the hydrobenzamide, citrate, and PVP-capped Sn particles. The figure shows that the particle sizes were similar to those estimated from XRD. In the case of the hydrobenzamide-capped Sn powder, the TEM image was obtained by mixing it with carbon black in NMP to examine the practical dispersity in the composite electrode. The hydrobenzamide-capped Sn nanoparticles showed good dispersity compared with the PVP- and citrate-capped Sn particles. On the other hand, the 2,4,6-tri(2-pyridyl)-1,3,5-triazine-, 3-(2-pyridyl)-5,6-diphenyl-1,2,4-triazine-

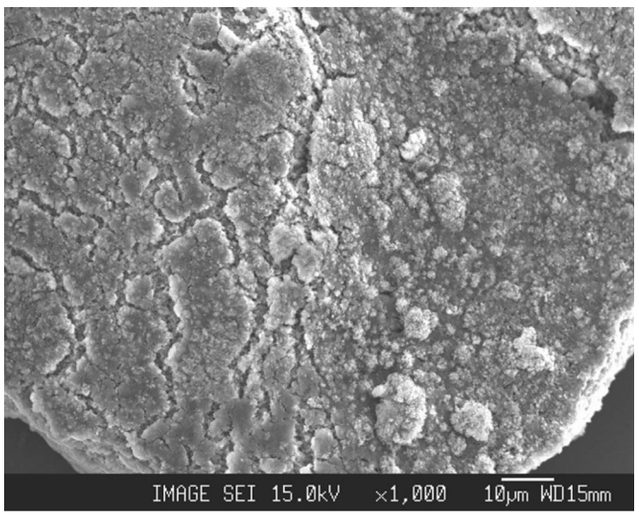

Figure 5. SEM image of the cycled PVP-capped Sn electrode.

capped Sn particles showed severe particle agglomeration in which the particle size was smaller than 200 nm.[24] In contrast to the Au and Ag nanoparticles capped with PVP and citrate, which showed a uniform distribution of ~50 nm-sized particles, the Sn particle with the same capping agents shows the aggregated particles with the sizes >100 nm. This indicates that PVP and citrate were not effective in controlling the particle growth and the enhanced Oswald ripening process. It should be noted that PVP produces faster particle growth than citrate, showing a particle size over ~300 nm.

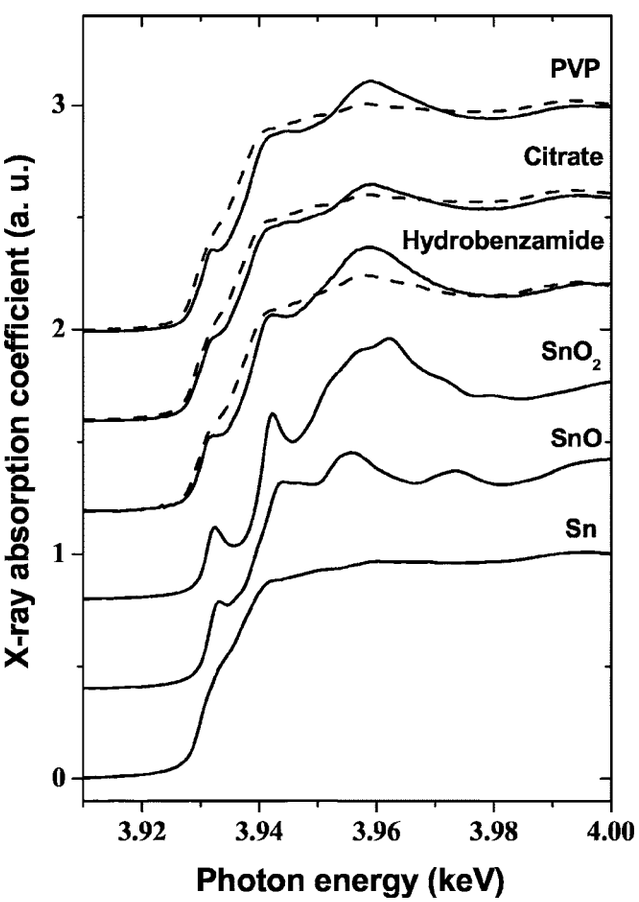

Figure 6. Normalized Sn L_{III}-edge XANES spectra for the hydrobenzamide-, PVP-, and citrate-capped Sn particles before (dashed line) and after 30 cycles (solid line).

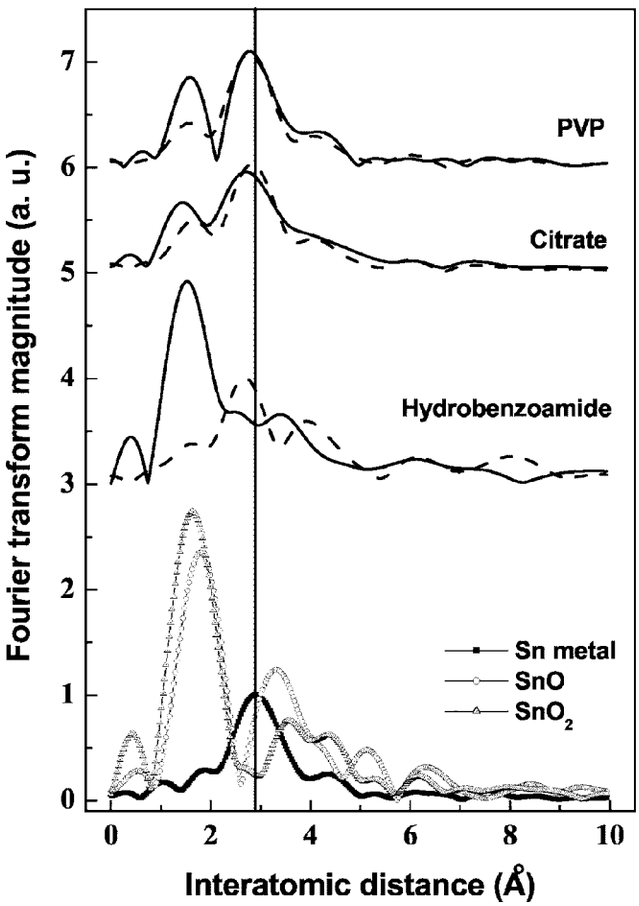

Figure 7. FT magnitudes (right) for hydrobenzamide-, PVP-, and citrate-capped Sn particles before (dashed line) and after 30 cycles (solid line).

Figure 3 shows the voltage profiles of the hydrobenzamide-, citrate-, PVP-capped Sn particles during the first cycle between 1.5 and 0 V at the rate of 0.1 C (1 C = 900 mA/g) in a coin-type half cell. The first charge capacities and irreversible capacity ratios of the hydrobenzamide-, citrate-, PVP-capped Sn particles were 1480, 1084, 1116 mAh/g, and 64, 74, 83%, respectively, showing that larger particles led to having a smaller irreversible capacity. As the particle size decreases, the initial irreversible capacity increased due to the enhanced side reactions with the electrolyte. However, the hydrobenzamide-capped Sn showed much improved capacity retention compared to the PVP and citrate capped Sn, showing 70% capacity retention after 30 cycles while that of the PVP and citrate-capped Sn shows 5% capacity retention. On the other hand, when the amount of hydrobenzamide in the course of sample preparation was decreased to half, the particle size was quite irregular and severely aggregated. This indicates that when the amount of disperser (capping agent) is insufficient, it cannot form a complete protection layer, and the particles will aggregate easily. With more disperser added, it can form a more perfect layer quickly, which protects the particles from agglomeration and growth. A higher cutoff voltage induced more aggregated Sn particles along with volume mismatch, resulting in capacity fading, and capacity retention was improved by 20% when the cutoff voltage of the cell containing PVP-capped tin anode was decreased to 1.2 V, compared with a 1.5 V cutoff.

In order to investigate the Sn particle growth after cycling, the

XRD patterns and TEM images of the cycled electrodes were examined. The estimated particle sizes of the hydrobenzamide-, citrate-, and PVP-capped Sn after cycling using XRD patterns were ~90, ~500, and ~500 nm, respectively, corresponding to a particle growth rate of 70, 400, and 140% of that before cycling, respectively (Fig. 1b). This result coincides with the TEM result in Fig. 4, and smaller particle growth of the PVP-capped Sn than citrate-capped Sn suggests that PVP is more effective in inhibiting particle growth during the cycling. Note that the hydrobenzamide-capped Sn shows loosely aggregated or somewhat separated tin particles, and separated tin particle shows particle growth to the size of ~80 nm. On the other hand, the citrate- and PVP-capped Sn showed a particle size of ~500 nm. In addition, PVP-capped Sn shows some portion of the cycled Sn exhibiting the formation of Sn fibers with a thickness of 100 nm. Figure 5 shows a scanning electron microscopy (SEM) image of the cycled PVP-capped Sn electrodes, showing severe cracks as a result of the substantial volume change during lithium alloying/dealloying. This is expected to lead to electrical isolation between the particles and result in capacity fading.

In order to investigate the effects of the capping agent on the electrochemical properties and structural variations in the Sn nanoparticles, Sn L_{III}-edge X-ray absorption spectroscopy was carried out before and after cycling. Figure 6 shows the normalized Sn L_{III}-edge X-ray absorption near-edge structure (XANES) spectra for the hydrobenzamide-, citrate- and PVP-capped Sn nanoparticles before and after cycling, compared with those of the reference materials. Before cycling, as shown in the XANES pattern in Fig. 6, all the Sn nanoparticles showed the characteristic peak features of metallic Sn. After cycling, the Sn L_{III}-edge XANES spectra changed. Although the overall peak features were similar to those of the Sn metallic state, the relative ratios of the pre-edge peak intensity were different. In particular, the hydrobenzamide-capped Sn nanoparticle shows peak features closer to that of SnO_2. However, it is certain that there is no oxidized Sn in the overall phase even if the hydrobenzamide-capped Sn has a similar oxidized state to the metallic Sn. The XRD pattern (Fig. 1b) confirmed the existence of a tetragonal β-Sn metallic phase after cycling and did not show the formation of SnO_2 or SnO phases. Therefore, the peak feature variation after cycling is believed to be due to the interaction between the surface Sn and the capping agent. Figure 7 shows Fourier transform (FT) magnitude of Sn L_{III}-edge EXAFS for hydrobenzamide-, citrate-, and PVP-capped Sn nanoparticles before and after cycling. The FT peak variations for the capping agents show there was no phase transition to any oxidized Sn but the distinct maintenance of the metallic Sn phase after cycling. For the capped Sn particles prior to cycling, there was an FT peak of Sn–Sn metallic bonding at the lower r space than that of the pure Sn particle at approximately 2.9 Å. Among them, the Sn–Sn bond for hydrobenzamide (2.69 Å) is shorter than those for PVP (2.85 Å) and citrate (2.80 Å). After cycling, the metallic peak features were retained in all the capping agents, with the generation of a FT peak at 1.56 Å showing Sn-L bonding in the surface region (L is ligand of capping agent). In particular, the hydrobenzamide-capped Sn shows the abrupt evolution of the FT peak with respect to the other capping agents. The peak feature variation in the hydrobenzamide-capped Sn after cycling can be explained by the strong coordination formed as a result of chemical bonding with the nitrogen of the hydrobenzamide capping agent. As the cycling proceeds, more surface Sn atoms are coordinated with the nitrogen of hydrobenzamide. The XANES peak feature like SnO_x after cycling mentioned above could be also explained with the increase of Sn–N bond. As the result, the hydrobenzamide capping has a greater influence on controlling the particle growth during cycling rather than citrate- and PVP-capped Sn nanoparticles.

Conclusions

Hydrobenzamide-capped Sn nanoparticles had a smaller particle size and showed better dispersity than the citrate and PVP-capped Sn. Moreover, they showed the best capacity retention despite the 36% irreversible capacity ratio. This result was consistent with a lower amount of particle agglomeration compared with the others.

Acknowledgments

We are grateful to the authorities at Pohang Light Source (PLS) for XAS measurements. The experiments at PLS were supported in part by Korea MOST and POSTECH. This work was supported by grant no. B1220-0501-0019 from the University Fundamental Research Program of the Ministry of Information and Communication in Republic of Korea.

Jaephil Cho assisted in meeting the publication costs of this article.

References

1. B. Wiley, Y. Sun, B. Mayers, and Y. Xia, *Chem.—Eur. J.*, **11**, 454 (2005).
2. C. N. R. Rao, A. Müller, and A. K. Cheetham, *Chemistry of Nanotechnologies*, Wiley-VCH, Weinheim (2004).
3. D. L. Feldheim and C. A. Foss, Jr., *Metal Nanoparticles*, Marcel Dekker, New York (2002).
4. C. Nayral, T. Ould-Ely, A. Maisonnat, B. Chaudret, B. P. Fau, L. Lescouzeres, and A. Peyre-Lavigne, *Adv. Mater. (Weinheim, Ger.)*, **1**, 61 (1999).
5. C.-S. Yang, Y. Q. Liu, and S. M. Kauzlarich, *Chem. Mater.*, **12**, 983 (2000).
6. Y. Wang, J. Y. Lee, and T. C. Deivaraj, *J. Electrochem. Soc.*, **151**, A1804 (2004).
7. Y. Wang, J. Y. Lee, and T. C. Deivaraj, *J. Mater. Chem.*, **14**, 362 (2004).
8. Z. S. Pillai and P. V. Kamat, *J. Phys. Chem. B*, **108**, 945 (2004).
9. Y. Sun, B. Mayers, and Y. Xia, *Nano Lett.*, **3**, 675 (2003).
10. Y. Sun and Y. Xia, *Adv. Mater. (Weinheim, Ger.)*, **14**, 833 (2002).
11. I. A. Courteny and J. R. Dahn, *J. Electrochem. Soc.*, **144**, 2045 (1997).
12. M. Winter and J. O. Besenhard, *Electrochim. Acta*, **45**, 31 (1999).
13. I.-S. Kim, G. E. Blomgren, and P. N. Kumta, *Electrochem. Solid-State Lett.*, **7**, A44 (2004).
14. M. Noh, Y. Kwon, H. Lee, J. Cho, Y. Kim, and M. G. Kim, *Chem. Mater.*, **17**, 1926 (2005).
15. J. Graetz, C. C. Ahn, R. Razami, and B. Fultz, *Electrochem. Solid-State Lett.*, **6**, A194 (2003).
16. M. Wachtler, J. O. Besenhard, and M. Winter, *J. Power Sources*, **94**, 189 (2001).
17. J. Yang, B. F. Wang, K. Kang, Y. Liu, J. Y. Xie, and Z. S. Wen, *Electrochem. Solid-State Lett.*, **6**, A151 (2003).
18. J. Yang, Y. Takeda, Q. Li, N. Imanishi, and O. Yamamoto, *J. Power Sources*, **90**, 64 (2000).
19. K. T. Lee, Y. S. Jung, and S. M. Oh, *J. Am. Chem. Soc.*, **125**, 5652 (2003).
20. Q. F. Dong, C. Z. Wu, M. G. Jin, Z. C. Huang, M. S. Zheng, J. K. You, and Z. G. Lin, *Solid State Ionics*, **167**, 49 (2004).
21. X. P. Gao, J. L. Bao, G. L. Pan, H. Y. Zhu, P. X. Huang, F. Wu, and D. Y. Song, *J. Phys. Chem. B*, **108**, 5547 (2004).
22. J. Xie, X. B. Zhao, G. S. Cao, Y. D. Zhong, M. J. Zhao, and J. P. Tu, *Electrochim. Acta*, **50**, 1903 (2005).
23. Y. Yang, M. Wachtler, M. Winter, and J. O. Besenhard, *Electrochem. Solid-State Lett.*, **2**, 161 (1999).
24. M. Noh, Y. Kim, M. Kim, H. Lee, H. Kim, Y. Kwon, Y. Lee, and J. Cho, *Chem. Mater.*, **17**, 3320 (2005).